

Supporting Information

Epitaxially Aligned Cuprous Oxide Nanowires for All-Oxide, Single-Wire Solar Cells

*Sarah Brittan,^{1,2} † Youngdong Yoo,¹ † Neil P. Dasgupta,^{1,3} Si-in Kim,⁴ Bongsoo Kim,⁴ and
Peidong Yang^{1,2*}*

† These authors contributed equally to this work.

¹Department of Chemistry, University of California, Berkeley, California 94720, United States.

²Materials Science Division, Lawrence Berkeley National Laboratory, 1 Cyclotron Road, Berkeley, California 94720, United States. ³Department of Mechanical Engineering, University of Michigan, Ann Arbor, Michigan 48109, United States. ⁴Department of Chemistry, KAIST, Daejeon 305-701, Korea.

* Please address correspondence to p_yang@berkeley.edu.

Synthesis and characterization of the Cu₂O nanowires

Fabrication of the single-wire solar cells

Optical and electrical measurements

Table S1: Electrical properties of the pristine and chlorine-exposed wires

Table S2: Electrical properties of the ZnO deposited by low-temperature ALD

Figure S1: XRD and facet identification of the chlorine-exposed wires

Table S3: Photovoltaic performance of the single-wire solar cells

Figure S2: SPCM of two single-wire solar cells

Synthesis and characterization of the Cu₂O nanowires

Cu₂O nanowires were synthesized in a horizontal hot-wall single-zone furnace with a 1-in. inner diameter quartz tube, equipped with a roughing pump and mass flow controllers. The copper slug (21.5 g, 99.9999 %, Sigma-Aldrich) was placed in an alumina boat at the center of the furnace. The substrates were placed a few centimeters downstream from the center. After evacuating the quartz tube in the furnace to less than 500 mTorr, the carrier gas (Ar) and 10 % O₂/Ar gas were supplied through mass flow controllers at rates of 200 sccm and 1 sccm (standard cubic centimeter per minute), respectively. The chamber pressure was maintained at 6 Torr. The copper slug was heated to 1140 °C at a rate of ~50 °C /min at the furnace's center, and the copper vapor was transported to the lower temperature region by the carrier gas, where Cu₂O nanowires were grown on the substrates. The temperature of the substrates was measured to be ~860 °C. The size of the MgO substrates (MTI Corporation, USA) was 5 mm × 5 mm, and the reaction time was 1 hour.

For the synthesis of chlorine-exposed Cu₂O nanowires, MgCl₂ powder (0.5 g, 99.99%, Sigma-Aldrich) was placed in an alumina boat a few centimeters upstream from the center of the furnace. The temperature of the MgCl₂ powder was about 150-200 °C. All other experimental conditions were the same as the conditions used to synthesize the pristine Cu₂O nanowires.

SEM images were taken on a JEOL JSM-6340F field-emission scanning electron microscope. XRD patterns were recorded on a Bruker D8 X-ray Diffractometer with a Cu source. Cross-sectional TEM specimens were prepared by a dual-beam focused ion beam (FEI Nova 600 NanoLab) equipped with a nanomanipulator (Kleindick MM3A). TEM and HRTEM images were taken on a TECNAI F30 TEM.

Fabrication of the single-wire solar cells

After growth of the wires, photolithography directly on the MgO substrate was used to pattern a contact on one end of the wire. Within 36 hours of developing the photoresist, the samples were loaded into the sputterer to deposit ~60 nm of platinum after pumping down for 3 hours to ensure a clean surface. Liftoff was performed in warm acetone. Samples held for several days before metallization exhibited non-ohmic contacts. No cleaning or etching steps were performed on the wires before metallization.

Next, the substrate was spin-coated with a bilayer of poly(methyl methacrylate) (PMMA) and i-line photoresist. The PMMA was estimated to be 300-500 nm thick. Photolithography was used to pattern the windows that would become the heterojunction, and O₂ plasma etching (3 mins, 50W, 180 mTorr) removed the PMMA using the patterned photoresist as a mask. After selectively removing the photoresist by soaking the chip in isopropanol for 20 mins, the PMMA was baked in rough vacuum (400 mTorr) at 90°C for 30 mins to remove any residual solvent. A final 30 s O₂ descum (same conditions as above) was used to clean the surface before deposition of the *n*-type layer; however, SEM images show that residual particles from the PMMA still remained.

Substrates then underwent low-temperature ALD of either ZnO (~30 nm) or ~10-20 nm of amorphous TiO₂ and then ZnO in a home-built ALD station. Such depositions had to be performed well below the glass temperature of PMMA (~120°C) to avoid damaging the lithographic patterning and to reduce heating of the oxide interface. ZnO deposition was performed using diethylzinc and water as precursors at 85°C. While its thickness varied between depositions, its carrier concentration and mobility were found to be consistent at $2-7 \times 10^{18} \text{ cm}^{-3}$

and 2-3 cm²/Vs. TiO₂ films were deposited at 100°C using tetrakis(dimethylamido)titanium(IV) as the titanium precursor at the Stanford Nanoprototyping Laboratory. Films deposited using the same precursor in the Stanford Nanofabrication Laboratory did not produce working devices.

After deposition of the films, the PMMA was lifted off by soaking the substrates in acetone at room temperature for 24 hours and then ultrasonicing for 30-180 s.

A third lithographic step was then used to pattern Ti/Au (10 nm/100-150 nm) contacts on the ZnO film. A 30-s O₂ plasma was used to prepare the ZnO before metallization, and liftoff was performed in warm acetone. No post-annealing treatments were required to achieve ohmic contact to the ZnO film.

Optical and electrical measurements

A 150 W xenon arc lamp (Newport Corp.) with an AM 1.5G filter was used to measure the nanowire's photovoltaic response. The light intensity was calibrated using a 2.4 mm × 2.8 mm silicon photodiode (Hamamatsu Corp.) referenced to a calibrated silicon photodiode (Newport Corp.). *I-V* characterization was performed with a Keithley 2636 source-measure unit (SMU).

The dependence of the photocurrent on wavelength (photocurrent spectrum) was obtained by measuring the current generated in the device at 10-nm increments, normalized by the photon flux of the source. A 300 W xenon arc lamp (Newport Corp.) was coupled to a monochromator (Newport Corp.) to obtain monochromatic illumination. The output of the source was measured using a 1.1 × 1.1 mm silicon photodiode (Hamamatsu Corp.) referenced to a calibrated silicon photodiode (Newport Corp.). Both the photodiode and the devices were positioned using a micrometer-driven translation stage (Thorlabs). The full-width, half-maximum of the monochromatic illumination was ~15 nm.

A home-built confocal microscope with piezoelectric scanning stage was used for simultaneous reflection imaging and scanning photocurrent mapping (SPCM). A helium-cadmium laser ($\lambda=442$ nm) or diode-pumped solid-state laser ($\lambda=532$ nm) was focused to a diffraction-limited spot through the microscope's objective lens (NA = 0.95). At each point in the reflection image, the photocurrent was recorded by a Keithley 236 source-measure unit. Photocurrent maps were plotted using MATLAB®, and the reflection images were processed using *Image SXM*.¹

1. Image SXM, S. D. Barrett. <http://www.ImageSXM.org.uk>. 2008.

Device	4-pt Resistance (M Ω)	Base's Width (nm)	Length (μ m)	Conductivity (mS)	Est. Carrier Conc. (cm ⁻³) (μ =100 cm ² /Vs)
1A	58.3	1420	0.97	0.47	2.9E+13
1B	40.1	1630	1.06	0.57	3.5E+13
1C	51.4	1520	0.75	0.36	2.3E+13
1D	35.8	1650	0.53	0.31	1.9E+13
1E	45.1	1560	0.77	0.40	2.5E+13
2A	111.2	1480	0.82	0.19	1.2E+13
CI A812	38.9	1013	0.60	0.87	5.4E+13
CI A821	90.4	889	1.07	0.85	5.3E+13
CI B821	63.1	1510	0.82	1.09	6.8E+13
CI C821	104.0	1282	0.87	0.77	4.8E+13
CI 808A12	61.5*	959	0.70	0.71	4.4E+13
CI 806A12	11.4*	702	0.74	7.51	4.7E+14
CI 806B12	86.8*	735	0.73	0.89	5.5E+13

Table S1. Electrical properties of the pristine (white) and chlorine-exposed wires (gray). Resistance was obtained with a linear fit to the device's I - V curve measured in the dark. Asterisks indicate that the measurement used two electrodes rather than four, so the actual conductivity/carrier concentration might be higher than measured. Conductivity was calculated from the resistance measurement and the geometry of the wire as measured in SEM. The estimated carrier concentration assumed the bulk mobility of Cu₂O (100 cm²/Vs).

Temp (°C)	Growth Rate Å/cycle	N (cm ⁻³)	Mobility (cm ² /Vs)
50	1.30	1.0E+15	0.1
65	1.58	1.0E+17	2.7
85	1.64	6.0E+18	2.8
150	1.66	1.4E+20	7.2

Table S2. Electrical properties of the ZnO deposited by low-temperature ALD. The mobility and carrier concentration (N) of the films increase with increasing deposition temperature, as determined by Hall-effect measurements of 25-45 nm films deposited on quartz substrates. 150°C is a standard deposition temperature for ALD ZnO; deposition at lower temperatures produces films with substantially lower carrier concentrations.

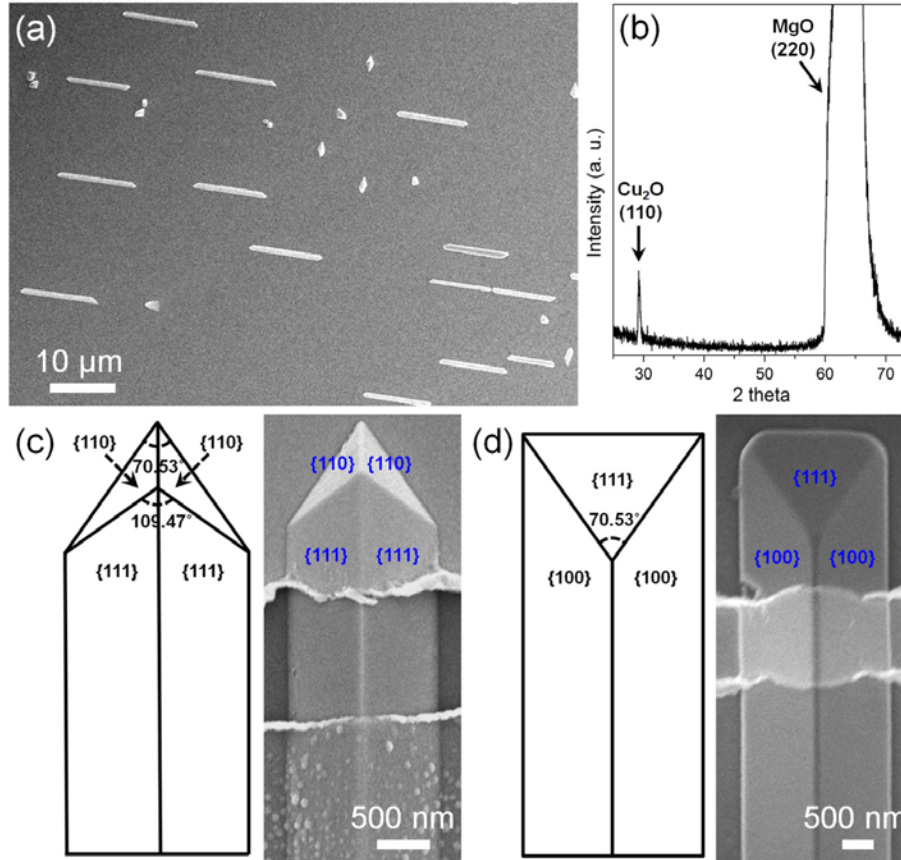


Figure S1. XRD and facet identification of the chlorine-exposed wires. (a) Top-view SEM image of the chlorine-exposed wires. (b) XRD pattern of the wires showing that Cu_2O is grown oriented on MgO (110). (c) Orthogonal projection image and top-view SEM image of a wire possessing $\{111\}$ side facets, $\{110\}$ tip facets, and a $\{110\}$ bottom plane. (d) Orthogonal projection image and top-view SEM image of a wire possessing $\{100\}$ side facets, a $\{111\}$ tip facet, and a $\{110\}$ bottom plane.

	V_{oc} (V)	I_{sc} (pA)	J_{sc} (mA/cm^2)	FF	P_{max} (pW)	Area (cm^2)	Efficiency (%)
A	0.24	197.7	4.3	0.37	18	4.6E-08	0.39
B	0.33	61.6	0.8	0.42	8.5	8.2E-08	0.10
D	0.03	25.6	0.1	0.26	0.2	2.2E-07	0.0009
E	0.36	25.0	0.6	0.27	2.4	4.4E-08	0.055
F	0.34	167.3	2.9	0.22	12.5	5.8E-08	0.22
H	0.30	20.8	0.3	0.27	1.7	6.0E-08	0.028
J	0.34	214.9	2.7	0.22	16.4	7.9E-08	0.21

Table S3. Photovoltaic performance of the single-wire solar cells fabricated from $\text{Cl-Cu}_2\text{O}/\text{TiO}_2/\text{ZnO}$ junctions. Areas were measured from SEM images, based on the entire core-shell region of the wire.

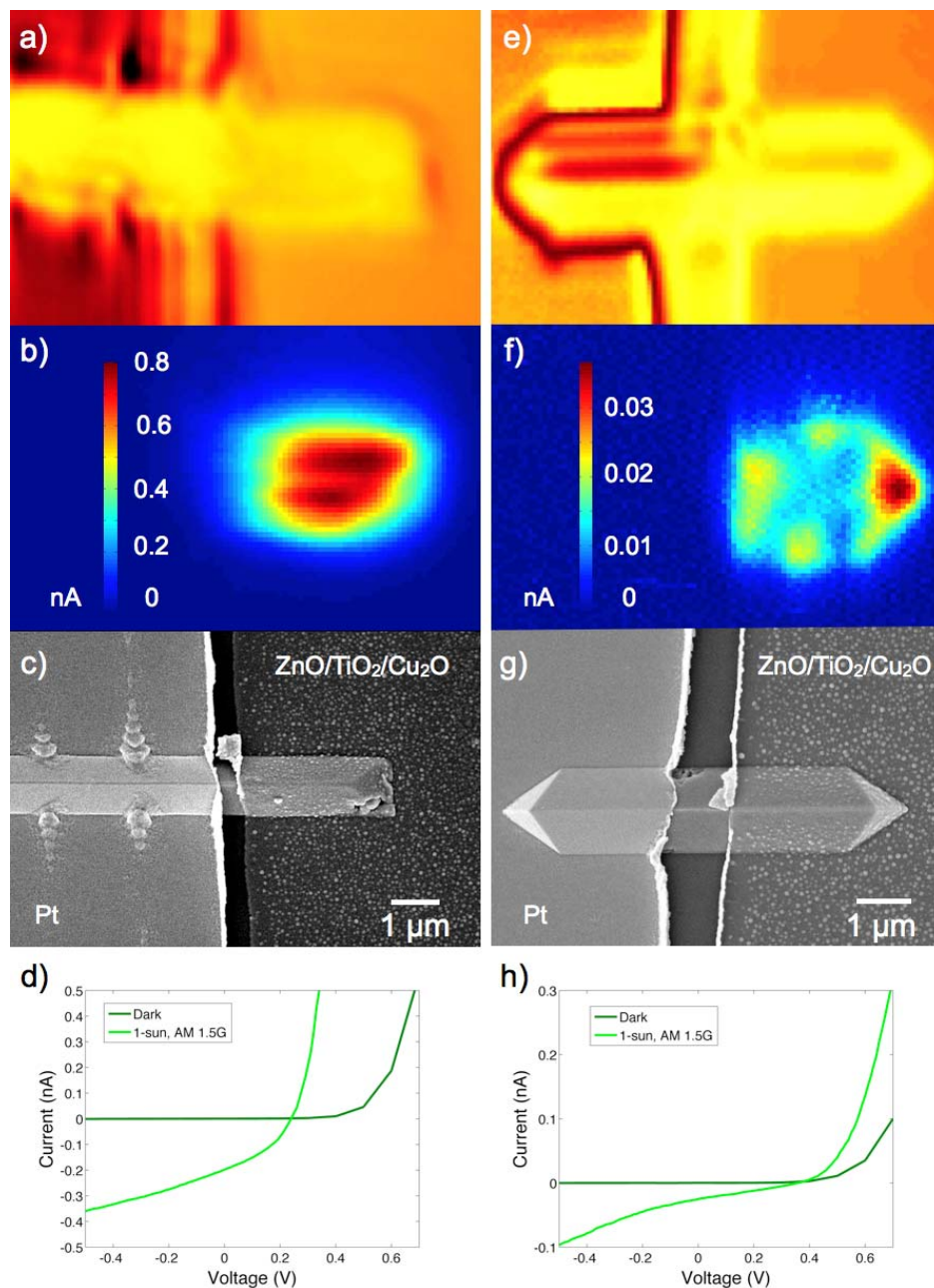


Figure S2. SPCM of two single-wire solar cells. Scanning reflection images (a,e) obtained simultaneously with the photocurrent maps (b,f), corresponding SEM images (c,g), and one-sun I - V curves (d,h) of device A (a-d) and device E (e-h), respectively ($\lambda=532$ nm). In the reflection images, red corresponds to the most reflective surfaces, while yellow indicates scattering or absorption. In the I - V curves, hysteresis has been removed for clarity. Typically in these and other devices, not all of the junction area was active. The increase in photocurrent near the tip of the wire in E might be from preferential in-coupling of the light at that point or from improved junction quality on those crystal facets, which are $\{110\}$.